VNU Journal of Science: Mathematics – Physics, Vol. 34, No. 4 (2018) 70-76

VNU Journal of Science: Mathematics - Physics

Journal homepage: https://js.vnu.edu.vn/MaP

# Synthesis and Electrochemical Properties of $Fe_2O_3$@C Composite

Bui Thi Hang*

*International Institute for Materials Science, Hanoi University of Science and Technology, Hanoi, Vietnam*

Received 14 December 2018
Revised 25 December 2018; Accepted 25 December 2018

**Abstract:** $Fe_2O_3$@C material was prepared by one-step hydrothermal method for use as a negative electrode in an iron-air battery. The structure of $Fe_2O_3$@C was determined by X-ray diffraction (XRD) measurement while their morphology was observed by scanning electron microscopy (SEM). The electrochemical properties of the $Fe_2O_3$@C electrode in alkaline solution were investigated using cyclic voltammetry (CV) measurement. The results showed that $Fe_2O_3$@C material with α-$Fe_2O_3$ structure and amorphous carbon were successfully synthesized by one-step hydrothermal method. CV measurements indicate that the redox reaction rate of the $Fe_2O_3$@C electrode is higher than that of the $Fe_2O_3$@AB electrode using commercial $Fe_2O_3$ and AB (Acetylene Black Carbon).

*Keywords:* $Fe_2O_3$@C material, $Fe_2O_3$@C electrode, hydrothermal method, iron-air battery.

## 1. Introduction

The demand for energy storage devices (batteries, supercapacitors...) has been increased rapidly due to their high energy density, long life, reasonable price [1-10]. Previous literatures have shown that metal/air batteries have higher theoretical energy density and specific energy but cheaper, safer than Lithium-ion batteries [7, 11-14]. However, the actual power density of this battery is still low. Therefore, metal/air batteries have been studying to increase their actual cycle performance and capacity. In metal/air battery, the metal is used as the negative electrode material contained in the battery and the oxygen is the positive electrode material that is dispersed into the battery from the air. Most metal/air batteries use aqueous electrolyte such as potassium hydroxide.

Among the metal/air batteries, iron/air batteries have received much attention due to their high theoretical energy, long life, high electrochemical stability, low cost and environmentally friendly [15]. However,

* Tel.: 84-978862528.
Email: hang@itims.edu.vn
https//doi.org/ 10.25073/2588-1124/vnumap.4307

iron/air batteries still have some limitations such as the instability of iron in the alkaline environment, the passive layer of $Fe(OH)_2$ formed during discharge and the evolution of hydrogen on the electrodes need to overcome before commercializing.

Our previous work has shown that carbon used as an additive for iron electrodes can increase its cyclability [17]. To overcome the shortcomings of the iron/air battery, $Fe_2O_3$@C powder was prepared by one-step hydrothermal method and used as electrode material in the iron/air battery to improve its cyclability and capacity.

## 2. Experimental

Mixture of 0.01 mol of $FeCl_3.6H_2O$ (China) dissolved 30ml of deionized water was slowly added into 15ml NaOH solution 2M to obtain a solution containing yellow-brown precipitation. The precipitates thus obtained were washed with distilled water several times to remove $Cl^-$ and $Na^+$ ions. Add 40ml of 2.5 M NaOH solution and 2.7 g of glucose to the precipitates and this mixture was stirred for 30 minutes, then keep at $160^0$C in 20 hours using autoclave. After hydrothermal process, the resulting yellow-brown solid was collected by filtration, washed with distilled water or alcohol several times. Subsequently, the product was dried at $60^0$C for 24h. The obtained compound was identified to be $Fe_2O_3$@C by X-ray diffraction (XRD). The morphology of the as-prepared $Fe_2O_3$@C powder was observed scanning electron microscopy (SEM).

To determine the electrochemical behavior of as-prepared $Fe_2O_3$@C, an electrode sheet was prepared by mixing 90 wt.% of the respective $Fe_2O_3$@C and 10 wt.% polytetrafluoroethylene (PTFE; Daikin Co.) and rolling. The electrodes were cut from electrode sheet into pellets with diameters of 1 cm. The electrode pellets were then pressed onto current collector Ti mesh with a pressure of about 150 kg $cm^{-2}$.

The $Fe_2O_3$/AB electrode sheet was prepared by the same procedure with the mixing ratio of $Fe_2O_3$:AB: PTFE = 45:45:10 wt. % ($Fe_2O_3$/AB:PTFE=90;10 wt.%) using Acetylene black (AB) of Denki Kagaku Co. Ltd. and $Fe_2O_3$ of Aldrich. $Fe_2O_3$/AB electrodes were made into a pellet of 1 cm diameter.

Cyclic voltammetry (CV) studies were carried out in a three-electrode glass cell assembly that had the synthesized material electrode as the working electrode, Pt mesh as the counter-electrode, and Hg/HgO as the reference electrode. The electrolyte was 8 mol $dm^{-3}$ KOH aqueous solution. CV measurements were taken at a scan rate of 5 mV $s^{-1}$ and within a range of –1.3 V to –0.1 V. In all electrochemical measurements, we used fresh electrodes without pre-cycling.

## 3. Results and discussion

*Structure and morphology of as-prepared material*

Figure 1 shows the XRD pattern of as-prepared material. The most typical peaks are characterized by (012), (104), (110), (113), (024), (116), (018), (214) and (300), corresponding to the values of 2θ (degree) at about 24.17, 33.19, 35.66, 40.90, 49.51, 54.13, 57.67, 62.49, and 64.05° respectively in the XRD diagram. They are characterized for a typical pattern of the $Fe_2O_3$ (ICSD No.82137). Thus, the as-prepared material is $Fe_2O_3$. No identifiable XRD signals related to carbon (ICSD No. 1079) are observed. This may be due to the carbon formed in the hydrothermal process has amorphous structure resulting in un-observable the diffraction peaks. To identify the formation of carbon, the SEM measurement was carried out and the result is shown in Fig. 2.

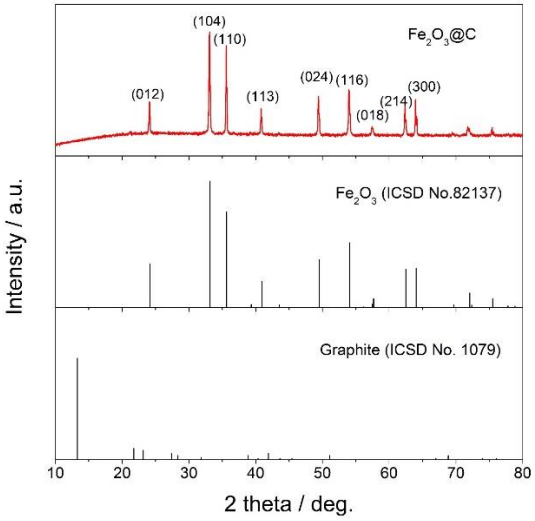


Figure 1. XRD pattern of the $Fe_2O_3$@C

It is clear that the particles with different shapes are covered by thin porous layers. The porous layers that surround the particles are carbon formed during the hydrothermal process while the inner particles are $Fe_2O_3$. These $Fe_2O_3$ particles have micrometer scale in size and un-uniform. The SEM measurement shows that $Fe_2O_3$@C with α- $Fe_2O_3$ structure and amorphous carbon were synthesized by hydrothermal method. From these XRD and SEM measurements, it can be concluded that the $Fe_2O_3$@C material was successfully fabricated by a one-step hydrothermal process.

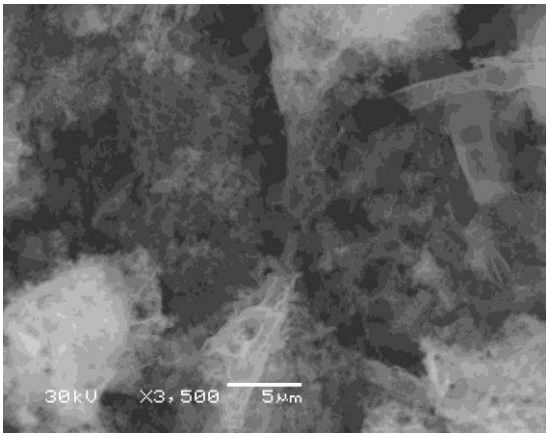


Figure 1. SEM image $Fe_2O_3$@C.

*Electrochemical properties*

To evaluate the quality of $Fe_2O_3$@C material synthesized by one-step hydrothermal process, CV measurement was performed at 5 initial cycles (notation 1,2,3,4 and 5) and the results are shown in Fig. 3.

On the forward scan from –1.3 V to –0.1 V, two small oxidation peaks were observed around – 1.0 V ($a_0$) and – 0.9 V ($a_1$) while one small reduction peak occurred around – 1.1V ($c_1$) together with hydrogen evolution at around – 1.2 V on the backward scan.

The previous investigation [18] indicated that the clear surface of iron was never exposed to the electrolyte, and over a partially oxidized surface, adsorption of hydroxyl ion takes place. The dissolution of the oxide or underlying metal by the ion transport through the oxide can also take place. The electrochemical reactions of iron in alkaline solution have been reported earlier as the following:

$$Fe + 2OH^- \underset{\text{Charge}}{\overset{\text{Discharge}}{\rightleftharpoons}} Fe(OH)_2 + 2e^- \quad (1)$$

$E^0 = –0{,}975$ V vs Hg/HgO [19]

$$Fe(OH)_2 + OH^- \underset{\text{Charge}}{\overset{\text{Discharge}}{\rightleftharpoons}} FeOOH + H_2O + e^- \quad (2)$$

$E^0 = –0{,}658$ V vs. Hg/HgO [19]

Và/hoặc

$$3Fe(OH)_2 + 2OH^- \underset{\text{Charge}}{\overset{\text{Discharge}}{\rightleftharpoons}} Fe_2O_3.4H_2O + 2e^- \quad (3)$$

$E^0 = –0{,}758$ V vs. Hg/HgO [18,20]

The first anodic peak $a_0$ can be attributed to oxidation of iron to $[Fe(OH)]_{ads}$, whereas the second anodic peak $a_1$ can be attributed to oxidation of $[Fe(OH)]_{ads}$ to $Fe(OH)_2$. The cathodic peak $c_1$ corresponds to the reduction of Fe(II) to Fe (Eqn. 1). Thus, $a_1$ and $c_1$ corresponds Fe/Fe(II) redox couple (Eqn. 1). The redox couple of Fe(II)/Fe(III) (Eqn. 2 and/or 3) was not observable. This could be ascribed to the insulating nature of the $Fe(OH)_2$ active material, which formed at $a_1$ peak would inhibit the Fe/Fe(II) redox couple, causing a large over potential.

However, the redox peaks $a_1$, $c_1$ are small, indicating that the redox reaction rate of Fe/Fe(II) (Equation 1) is very slow. This may be due to the porous carbon layer, which surrounds the iron oxide particles prevents the oxidation of iron, leading to slower reaction rate, reducing the cyclability of $Fe_2O_3$@C.

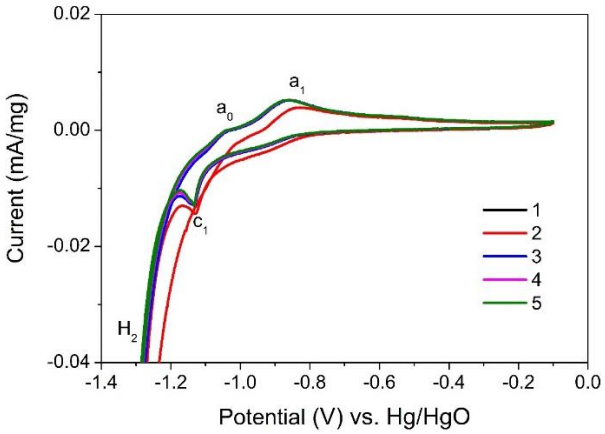


Figure 2. Cyclic voltammetry of $Fe_2O_3$@C electrode with $Fe_2O_3$@C:PTFE = 90:10 wt.% in KOH solution

To fully evaluate the applicability of synthesized $Fe_2O_3$@C, we subjected $Fe_2O_3$/AB electrode using commercial $Fe_2O_3$ (Aldrich) and AB carbon (Denki Kagaku Co.Ltd.) for CV measurement to compare with $Fe_2O_3$@C. Figure 4 depicts the SEM images of the commercial AB, $Fe_2O_3$ and $Fe_2O_3$/AB powder. The CV profiles of the $Fe_2O_3$/AB electrode are shown in Fig. 5.

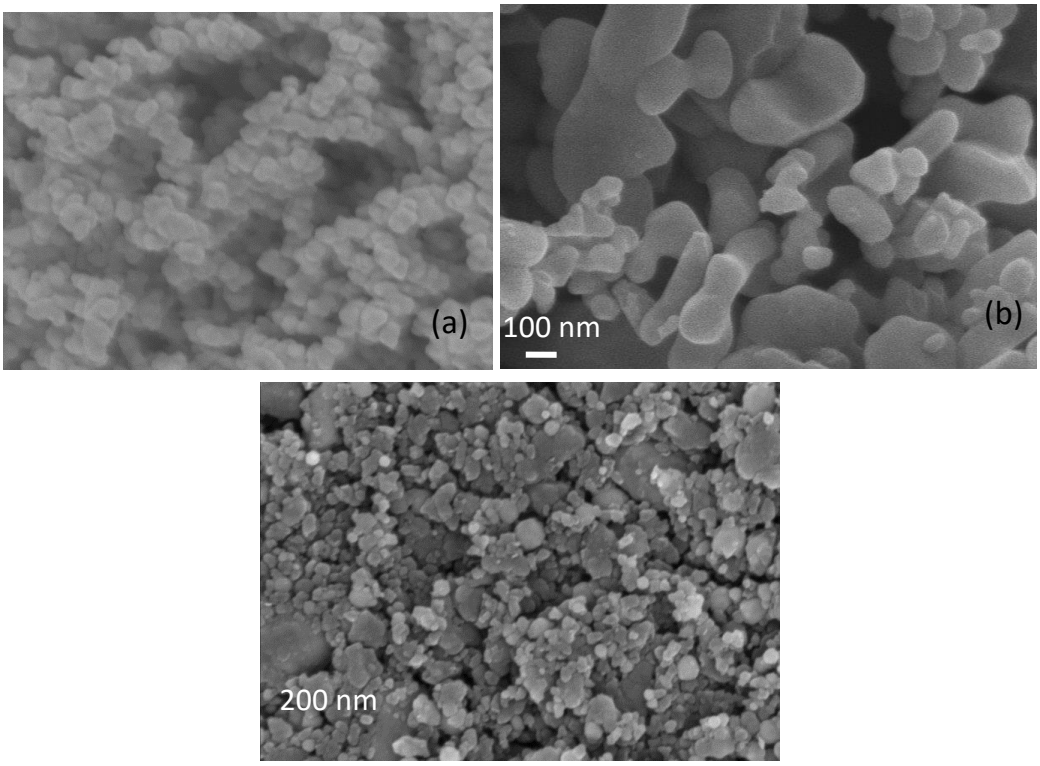


Figure 4. SEM images of commercial (a) AB powder, (b) $Fe_2O_3$ powder and (c) $Fe_2O_3$/AB mixture

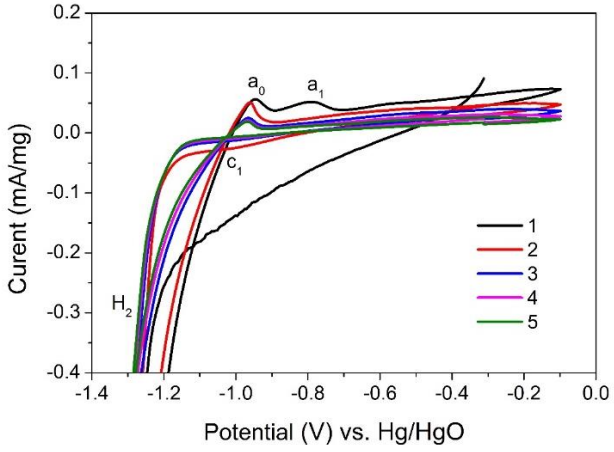


Figure 5. Cyclic voltammetry of $Fe_2O_3$/AB electrode with $Fe_2O_3$/AB:PTFE = 90:10 wt.% in KOH solution

SEM image of $Fe_2O_3$/AB (Fig. 4) is quite different to that of $Fe_2O_3$@C (Fig. 2). It is impossible to distinguish $Fe_2O_3$ and AB particles. This suggests that $Fe_2O_3$ and AB was mixed relative uniformly.

Comparison of the CV results of the $Fe_2O_3$@C electrode (Fig. 3) with those of $Fe_2O_3$/AB electrode at corresponding ratio of $Fe_2O_3$ and AB (Fig. 5) indicates that the redox peaks of $Fe_2O_3$@C appear more clearly, the reduction peak $c_1$ is separated from hydrogen evolution while in the $Fe_2O_3$/AB electrode the redox peaks are lower, the reduction peak $c_1$ completely covered by hydrogen evolution.

This is a positive behavior of the $Fe_2O_3$@C material synthesized by hydrothermal process compared to commercial materials. However, the redox current of the $Fe_2O_3$@C electrode is still low. It may be due to the porous carbon layers surrounded the iron oxide particles inhibit the oxidation of iron, leading to slowdown redox reaction rate. To overcome this phenomenon, the carbon layer formed during the hydrothermal process has to be optimized to increase the cyclability of iron oxide. Consequently, the $Fe_2O_3$@C material synthesized by this method needs to be further improved to meet the demands for iron-air battery. These steps will be carried out in the subsequent studies.

## 4. Conclusion

$Fe_2O_3$@C material has been successfully synthesized by one-step hydrothermal method. Their structure, morphology and electrochemical characteristics were investigated by XRD, SEM and CV measurement. The XRD and SEM results showed that the $Fe_2O_3$@C material with α- $Fe_2O_3$ particles covered by amorphous porous carbon was prepared by a simple hydrothermal method, easy to fabricate large amount of material for practical application. Electrochemical measurements indicate that $Fe_2O_3$@C obtained by hydrothermal process has better cyclability than $Fe_2O_3$@AB commercial material at corresponding iron oxide and carbon ratio.

## Acknowledgment

This research is funded by Vietnam National Foundation for Science and Technology Development (NAFOSTED) under grant number 103.02-2018.04.

## References

[1] Westinghouse Advanced Energy Systems Division, and demonstration of a nickel/ iron battery for electric vehicle propulsion, J. Power Sources 11, (1984) 315.

[2] Eagle-Pitcher Industries Inc., Research, development, and demonstration of a nickel/ iron battery for electric vehicle propulsion, J. Power Sources 11, (1984) 316.

[3] A.A. Kamnev, The role of lithium in preventing the detrimental effect of iron on alkaline battery nickel hydroxide electrode: A mechanistic aspect, Electrochim. Acta 41 (1996) 267.

[4] J.G. Zhang, P.G. Bruce and X. G. Zhang, Handbook of Battery Materials - Chapter 22: Metal-Air Batteries, (2013) 1000.

[5] D. Zhou, W.L. Song, X. Li, L.Z. Fan and Y. Deng, Tin nanoparticles embedded in porous N-doped graphene-like carbon network as high-performance anode material for lithium-ion batteries, J. Alloys Compd. 699 (2017) 730.

[6] E.J. Rudd and D. W. Gibbons, High energy density aluminum/oxygen cell, J. Power Sources 47 (1994)329.

[7] K. Vijayamohanan, T.S. Balasubramanian and A.K. Shukla, Rechargeable alkaline iron electrodes, J. Power Sources 34 (1991) 269.

[8] A.K. Manohar, S. Malkhandi, B. Yang, C. Yang, G. K Surya Prakash. and S.R. Narayanan, A High-Performance Rechargeable Iron Electrode for Large-Scale Battery-Based Energy Storage, J. Electrochem. Soc. 159 (2012) A1209.

[9] G.M. Ehrlich, Lithium-Ion Batteries, Handbook of Batteries, (2002) 35.1.

[10] N. Nitta, F. Wu, J.T. Lee and G. Yushin, Li-ion battery materials: present and future, Mater. Today 18 (2014) 252.

[11] Anon, Iron-air batteries for electric vehicles, J. Power Sources 5 (1980) 344.

[12] L. Öjefors, Self-discharge of the alkaline iron electrode, Electrochim. Acta 21, (1976) 263.

[13] K.F. Blurton and A.F. Sammells, Metal/air batteries: Their status and potential - a review, J. Power Sources 4 (1979) 263.

[14] M. Lübke, N.M. Makwana, R.Gruar, C. Tighe, D. Brett, P. Shearing, Z. Liu and J.A. Darr, High capacity nanocomposite $Fe_3O_4$/Fe anodes for Li-ion batteries, J. Power Sources 291 (2015) 102.

[15] U. Casellato, N.Comisso and G. Mengoli, Effect of Li ions on reduction of Fe oxides in aqueous alkaline medium, Electrochim. Acta 51 (2006) 5669.

[16] T.S. Balasubramanian and A.K. Shukla, Effect of metal-sulfide additives on charge/discharge reactions of the alkaline iron electrode, J. Power Sources 41 (1993) 99.

[17] B.T. Hang, M. Egashira, I. Watanabe, S. Okada, J. Yamaki, S.H. Yoon, I. Mochida, The effect of carbon species on the properties of Fe/C composite for metal-air battery anode, J. Power Sources 143 (2005) 256.

[18] K. Micka, Z. Zabransky, Study of iron oxide electrodes in an alkaline electrolyte, J. Power Sources 19 (1987) 315.

[19] C. Chakkaravarthy, P. Periasamy, S. Jegannathan, K.I. Vasu, The nickel/iron battery, J. Power Sources 35 (1991) 21.

[20] J. Černý and K. Micka, Voltammetric study of an iron electrode in alkaline electrolytes, J. Power Sources 25(2) (1989) 111.